Heliyon 10 (2024) e40102

Contents lists available at ScienceDirect

Heliyon

journal homepage: www.cell.com/heliyon

Research article

Polarization-selective metamaterial absorber using tailored Y-shaped SRR for UWB device and Doppler navigation aids applications

Sayed Mahmud [a,***], Apurba Ray Chowdhury [a], Saif Hannan [a,**], Mohammad Tariqul Islam [b,*], Ahmed S. Alshammari [c], Mohamed S. Soliman [d,e]

[a] Department of Electronic and Telecommunication Engineering, International Islamic University Chittagong (IIUC), Chattogram 4318, Bangladesh
[b] Department of Electrical, Electronic and Systems Engineering, Faculty of Engineering and Built Environment, Universiti Kebangsaan Malaysia, Bangi 43600, Malaysia
[c] Department of Electrical Engineering, College of Engineering, University of Ha'il, Ha'il 81481, Saudi Arabia
[d] Department of Electrical Engineering, College of Engineering, Taif University, Taif 21944, Saudi Arabia
[e] Department of Electrical Engineering, Faculty of Energy Engineering, Aswan University, Aswan 81528, Egypt

ARTICLE INFO

Keywords:
Metamaterial absorber
Co & cross polar
Near zero refractive index metamaterial
Polarization selective
Doppler navigation

ABSTRACT

In this paper, we present an unprecedented metamaterial absorber design exhibiting exceptional characteristics in electromagnetic wave absorption. The proposed bent Y-shaped structure, fabricated on an FR-4 substrate with copper patches, showcases remarkable performance across a diverse frequency spectrum. Through exhaustive simulations in CST, this design manifests eight distinct resonant frequencies, achieving absorption rates exceeding 90 % at each resonance. The resonances, strategically spanning from L-band (3.728 GHz) through S-band, C-band, X-band, Ku-band, and K-band up to 22.664 GHz, signify unparalleled versatility and efficacy in mitigating electromagnetic radiation. It investigates the equivalent circuit parameters of a proposed metamaterial absorber design, focusing on inductance (L), capacitance (C), and resistance (R). This paper investigates the applications of UWB devices at 3.728 GHz and Doppler navigation aids at the 13.4 GHz frequency as regulated by the Federal Communications Commission. It includes a discussion on near-zero refractive Index Metamaterials (NZRIM), highlighting their potential utilization in achieving extraordinary control over wave behaviour. Notably, the absorber's inherent polarization insensitivity fortifies its adaptability in various applications. Additionally, the metamaterial exhibits near-zero or negative permittivity, altering electric response, while simultaneously demonstrating permeability absolute zero throughout all frequency bands sparking new avenues for exploration and challenging conventional electromagnetic theories.

* Corresponding author.
** Corresponding author.
*** Corresponding author.
E-mail addresses: sayedmahamudsijann@gmail.com (S. Mahmud), apurbaraychowdhury.ac.bd@gmail.com (A.R. Chowdhury), sh@iiuc.ac.bd (S. Hannan), tariqul@ukm.edu.my (M. Tariqul Islam), ahm.alshammari@uoh.edu.sa (A.S. Alshammari), soliman@tu.edu.sa (M.S. Soliman).

https://doi.org/10.1016/j.heliyon.2024.e40102
Received 9 August 2024; Received in revised form 1 November 2024; Accepted 1 November 2024
Available online 8 November 2024

1. Introduction

Metamaterials have garnered substantial attention for their extraordinary electromagnetic properties and their potential to revolutionize various technological domains. In this study, we present a comprehensive analysis of a novel metamaterial absorber design exhibiting unprecedented multi-resonance characteristics and exceptional absorption capabilities across a broad frequency range. This design features a sophisticated patch structure with intricate cuts and a dielectric gap, influencing the capacitance component of the equivalent circuit. By leveraging surface current analysis and geometric equations, we calculate the inductance and capacitance values, providing insights into the resonant behaviour of the absorber [1]

Ultra-wideband technology has been the focus of extensive research due to its wide frequency range (3.1 GHz–10.6 GHz), high data transfer rates, and precise localization capabilities. Our novel metamaterial absorber, designed with high absorption efficiency at multiple resonant frequencies, aligns well with UWB applications. This study explores the integration of the absorber in UWB devices and its potential to improve performance by minimizing interference and enhancing signal clarity. Also, Doppler navigation aids play a crucial role in aviation and maritime navigation by providing accurate measurements of speed and direction using the Doppler effect. Our novel metamaterial absorber, designed with high absorption efficiency at multiple resonant frequencies, aligns well with these applications. This study explores the integration of the absorber in UWB devices and its potential to improve performance by minimizing interference and enhancing signal clarity. Additionally, the resonant frequency at 13.4 GHz demonstrates its application in Doppler navigation aids, providing accurate and reliable navigation data. In many wireless communication systems, managing signal polarization is critical for efficient transmission and reception. However, traditional absorbers often lack polarization selectivity, leading to challenges in mitigating interference caused by unwanted polarizations. This limitation poses a significant problem in scenarios where signal integrity is crucial, and interference needs to be minimized. Absorbing both co-polarized and cross-polarized waves simultaneously might result in interference or crosstalk between the polarizations. This interference can distort the signals or degrade the quality of the received information.

Radar systems, such as those in the C-Band, rely on high-frequency waves to detect objects, commonly used in weather forecasting, air traffic control, and military surveillance. The MMA reduces radar cross-section (RCS) by absorbing incoming radar waves, enhancing stealth capabilities. Negative permittivity helps the absorber resonate at specific frequencies, improving its absorption efficiency in radar applications, and making it suitable for systems requiring low reflection and high Absorption. Electromagnetic Interference (EMI) shielding is critical in environments with high EM activity, like data centres and medical facilities. The MMA attenuates unwanted EM waves, ensuring sensitive electronic devices function without disruption. High absorption efficiency, reflected in a higher FOM, makes MMA effective for EMI shielding, preserving signal integrity in shielded environments. Microwave imaging systems use high-frequency waves to create images for medical diagnostics, security, and non-destructive testing. The MMA minimizes background reflections, enhancing image clarity and resolution by ensuring that only relevant reflections are captured. A near-zero refractive index further minimizes wave distortion, enhancing image quality by absorbing unwanted signals. In aerospace and defence, reducing RCS is crucial for stealth. The MMA absorbs radar waves, making military assets like stealth aircraft and naval vessels less detectable. Negative permittivity aids in resonating with radar frequencies, while high Absorption ensures that reflected signals are minimal, enhancing stealth capabilities. Satellite communications, particularly in the Ku-Band, require precise signal transmission. MMAs minimize distortion and interference, improving signal integrity. A near-zero refractive index reduces signal bending, ensuring efficient signal reception in satellite and Doppler navigation systems, making them ideal for high-frequency satellite communication systems. High-frequency antennas in the K-Band, used for radar and space communications, benefit from MMA's ability to absorb stray signals, enhancing performance and signal clarity. The moderate FOM ensures a balance between absorption efficiency and minimal signal loss, which is essential for maintaining high-resolution radar and communication system performance. 5G networks operate in high-frequency bands like the K-Band, offering faster data rates and low latency. MMA helps manage interference by absorbing reflections from surrounding surfaces, improving signal clarity and reducing latency. Positive permittivity ensures efficient Absorption of stray signals, enhancing 5G infrastructure performance.

In communication systems, it can effectively absorb unwanted co-polarized signals, reducing interference and enhancing signal quality by allowing desired polarizations to transmit with less interference. By selectively absorbing co-polarized waves, the absorber can enhance the overall efficiency of communication systems, minimizing power losses due to interference. In scenarios where crosstalk due to unwanted polarizations affects system performance, your selective absorber could mitigate this issue, leading to cleaner signal reception and transmission. The absorber's specific polarization selectivity could enable engineers to fine-tune and control signal polarization, optimizing antenna designs or polarization-sensitive devices within communication networks [2]. The quest for efficient electromagnetic wave absorbers has intensified with the increasing demand for electromagnetic interference (EMI) shielding, stealth technology, and wireless communication systems. Traditional absorber designs often struggle to achieve high absorption rates over multiple frequency bands. However, our proposed bent Y-shaped metamaterial absorber, engineered on an FR-4 dielectric substrate with precisely crafted copper patches, defies conventional limitations by manifesting remarkable performance across a diverse frequency spectrum.

Through extensive simulations utilizing CST Microwave Studio, our investigation reveals a distinctive feature set. This includes the manifestation of eight distinct resonant frequencies ranging from 3.728 GHz to 22.664 GHz, each accompanied by absorption rates

exceeding 90 %. The ability to attain such high absorption levels across this wide frequency span marks a significant departure from conventional absorber designs and underlines the versatility and efficacy of the proposed metamaterial structure. Moreover, the inherent polarization insensitivity of our absorber presents an outstanding attribute, enhancing its adaptability across various polarization states—an attribute rarely achieved in traditional absorber configurations. Notably, the observation of permeability absolute zero throughout all resonant band's challenges established electromagnetic theories and opens intriguing avenues for further exploration and theoretical refinement [3]. This study modifies a conventional bent Y-shaped metamaterial absorber, a strategically placed square-shaped cut in the centre of the ground copper element. This design alteration renders the absorber polarization-independent, achieving perfection in Absorption for both co and cross-polarizations. The impetus behind this modification stems from the pursuit of versatile absorbers capable of seamlessly adapting to various polarization states. By strategically incorporating the square-shaped cut, the absorber transcends conventional limitations, highlighting adaptability across a broad frequency spectrum. Theoretical insights into the electromagnetic interactions within this modified structure underpin its unique resonant behaviours, facilitating high absorption rates. This paper aims to elucidate the profound implications of these findings and explores the potential applications of the proposed metamaterial absorber in diverse fields such as telecommunications, radar technologies, and electromagnetic compatibility. By examining and understanding the unique resonant behaviours and polarization-independent nature of this metamaterial absorber, we anticipate paving the way for transformative advancements in absorber design and electromagnetic wave manipulation [4].

2. Basics of the proposed absorber

2.1. Basic absorption mechanisms

Metamaterial absorbers exploit resonant phenomena to achieve high absorption rates at specific frequencies. Resonance occurs when the dimensions and configurations of metamaterial structures match the incident wavelength, leading to maximum interaction and Absorption of the incoming waves. Multiple resonances can be engineered within a single metamaterial structure, allowing for Absorption across a broad frequency spectrum. Advanced metamaterial absorbers aim for polarization-insensitive characteristics, ensuring consistent absorption rates regardless of the incident wave's polarization. Wide-angle Absorption refers to the ability of a metamaterial absorber to efficiently absorb waves arriving from various incident angles, enabling versatility in practical applications.

Absorption in metamaterials occurs due to various mechanisms such as ohmic losses, dielectric losses, and magnetic losses. Ohmic losses result from resistive components within the metamaterial structure, causing energy dissipation in the form of heat when an electromagnetic wave passes through. Dielectric losses stem from energy dissipation within the dielectric material used in the metamaterial, leading to partial Absorption of incident waves. Magnetic losses arise from magnetic components within the metamaterial, where energy is absorbed due to hysteresis or magnetic resonance effects [5]. Achieving near-zero or perfect Absorption involves tailoring metamaterial structures to minimize reflection and maximize Absorption across the operating frequency band. Metamaterial designs with near-unity Absorption are essential for applications demanding high absorption rates and low reflectance, such as antennas, stealth technology, and sensing devices. If an absorber can stop electromagnetic waves from bouncing back or passing through, it means it's absorbing them perfectly. This perfect Absorption can be explained using equation 1

$$A(\omega) = 1\text{-}|\,S_{11}(\omega)|^2 \text{ - } |S_{21}(\omega)|^2 \tag{1}$$

where, $|S_{11}(\omega)|^2$ represents how much of the wave gets reflected, and $|S_{21}(\omega)|^2$ shows how much gets transmitted. Since the design uses a copper ground, which is an excellent conductor, very little of the wave will pass through the absorber. Additionally, the reflection of the incoming wave from the absorber is very small, as shown in Equation (2).

$$S_{11}(\omega) = \sqrt{\frac{Z_{MM}\omega) - Z_0}{Z_{MM}(\omega) + Z_0}} \tag{2}$$

Where, Z_{MM} is like the resistance of the MM absorber, and Z_O is the resistance in open space. We can describe the Z_{MM} which is the resistance of the MM absorber.

$$Z_{MM} = \sqrt{\frac{\mu_0\mu_r}{\varepsilon_0\varepsilon_r\,(\omega)}} \tag{3}$$

Here, μ_0 and $\in_0$ are the permeability and permittivity constant of free space, and μr (ω) and r (ω) are the frequency-dependent relative permeability and relative permittivity, respectively. Hence, free space impedance,

$$Z_O = \sqrt{\frac{\mu_0}{\varepsilon_0}} \approx 377\Omega \tag{4}$$

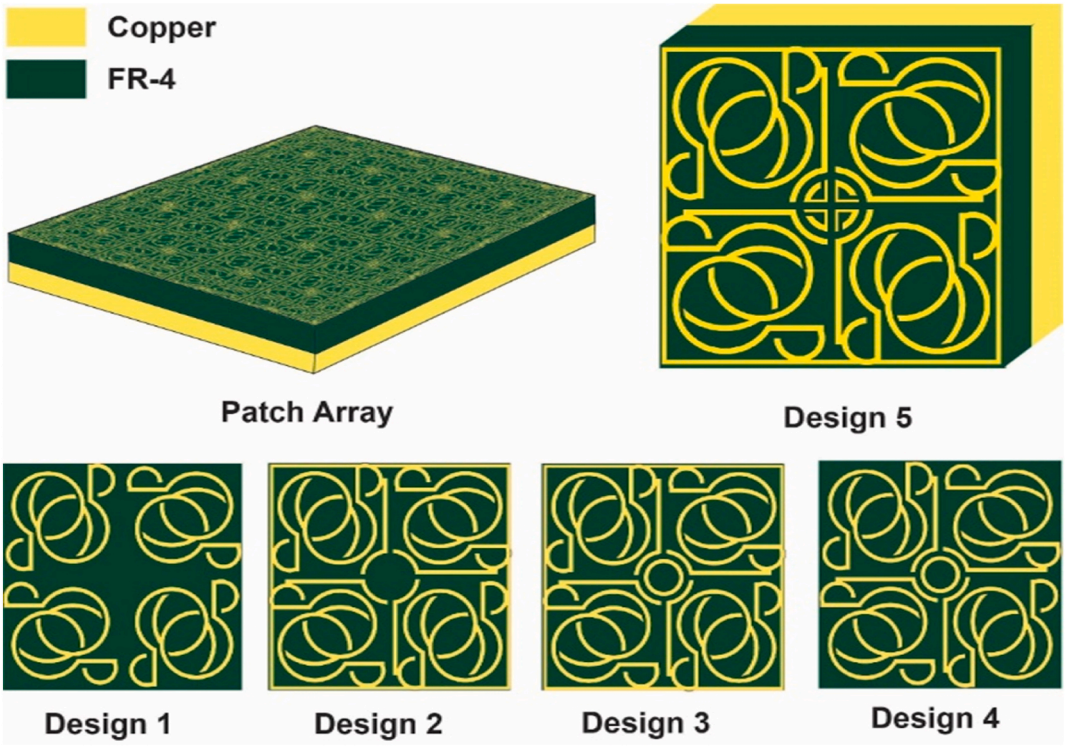

(a) Design

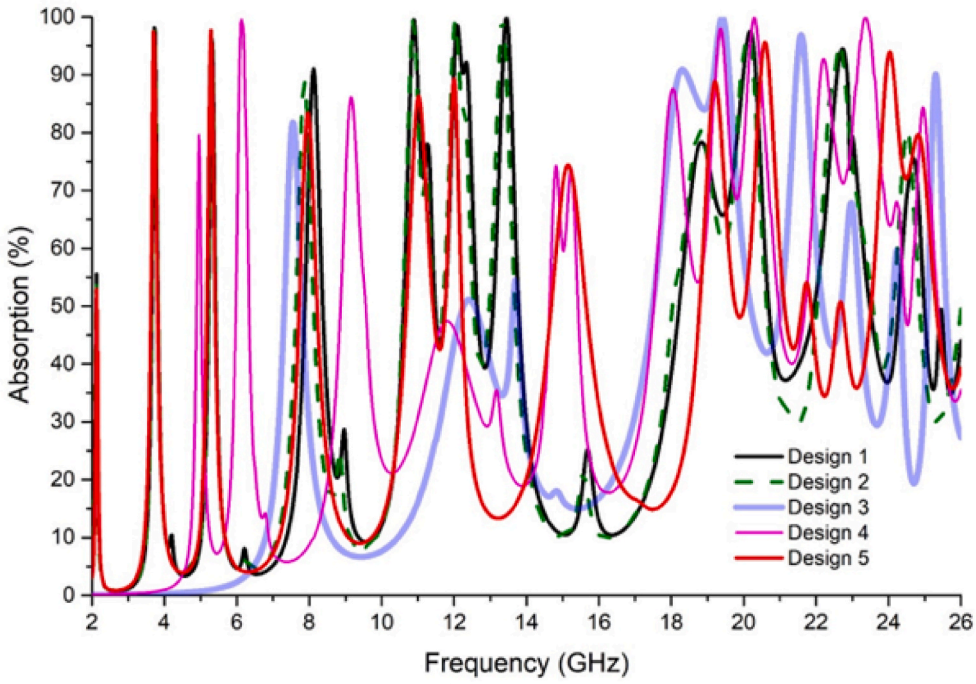

(b) Absorption

Figure-1. Design evaluation.

The co-polarization absorption behaviour of a metamaterial absorber is rooted in its unique structural design and electromagnetic interactions. It efficiently captures and dissipates co-polarized waves by aligning incident electromagnetic waves with the absorber's primary axis. The absorber's geometry influences surface currents, enhancing absorption efficiency. Impedance matching ensures optimal absorption rates by facilitating efficient dissipation of co-polarized electromagnetic energy. Optimization of patch dimensions and spacing achieves desired co-polarization absorption characteristics [6].

The cross-polarization absorption behaviour of a metamaterial absorber is defined by its ability to efficiently absorb electromagnetic waves with electric field vectors perpendicular to its primary axis. This characteristic is crucial for scenarios with variable incident wave polarizations, requiring the absorber to adapt and attenuate energy effectively in cross-polarized scenarios. The absorber's design enables it to adeptly capture energy from diverse polarization states, showcasing versatile cross-polarization absorption. Altered surface current distribution, a result of the modified design, enhances coupling with cross-polarized waves, allowing the absorber to capture energy from various polarizations. This cross-polarization absorption capability suits environments with mixed or changing polarization states, making it valuable for applications requiring adaptability to diverse communication signals or radar emissions [7].

2.2 Unit cell structure design

The primary objective of this research is to develop a multi-resonance Polarization selective metamaterial absorber exhibiting a minimum of 8 distinct resonance frequencies within a specified frequency range (L-band, S-band, C-band, X-band, Ku-band, and K-band). The absorber is engineered to achieve exceptionally high absorption efficiency at each resonance frequency aiming for values exceeding 90 %. The envisaged applications span across various fields such as electromagnetic interference (EMI) shielding, stealth technology, wireless communication systems, radar technologies, and electromagnetic compatibility [8]. Copper, renowned for its excellent electrical conductivity and ease of fabrication, was chosen for the patch and ground layers. FR-4, with its moderate dielectric constant, low cost, and compatibility with printed circuit board (PCB) fabrication techniques, was selected as the dielectric substrate.

Adopted a three-layer structure comprising a top copper patch layer, a middle FR-4 substrate layer with a thickness of 1.6 mm, and a bottom copper ground layer with a height of 0.035 mm. Unveiled a unique bent Y-shaped design for the absorber, never previously explored or developed. Designed the specific geometry of the copper patches to achieve the desired multi-resonance behaviour and polarization insensitivity. Controlled substrate and ground dimensions 10 × 10 mm to influence impedance matching and absorption bandwidth. Observed permeability absolute zero across all bands, challenging conventional electromagnetic theories [9]. Leveraged CST Microwave Studio for comprehensive simulations, exploring a myriad of design parameters. Investigated and iteratively refined parameters including patch dimensions (length, width, shape), substrate thickness, spacing between patches, theta, and phi angles to achieve and validate the multi-resonance characteristics and high absorption rates consistently. Observed consistent results across various simulations, showing polarization insensitivity. Characterized the absorption performance using simulation software, corroborating results through measured absorption spectra. Observed and confirmed the resonance frequencies of 3.728 GHz–22.664 GHz and absorption rates exceeding 90 % across all resonant bands as anticipated.

The initial design started with the basic Y-shaped SRR, which was selected for its proven ability to produce multiple resonances across a broad frequency range. To further improve the electromagnetic performance, we introduced several geometric modifications. We added a central circle and a square divider between the Y-shaped structure in the patches. These additions were aimed at enhancing the surface current distribution and achieving better resonance behaviour across the desired frequency bands. The central circle served as an additional resonating element, fine-tuning the inductive and capacitive interactions within the structure, while the square divider helped improve absorption efficiency by confining electromagnetic fields, thereby increasing polarization insensitivity and absorption rates. Next, we experimented with removing the square border to observe its impact on the absorption performance and polarization

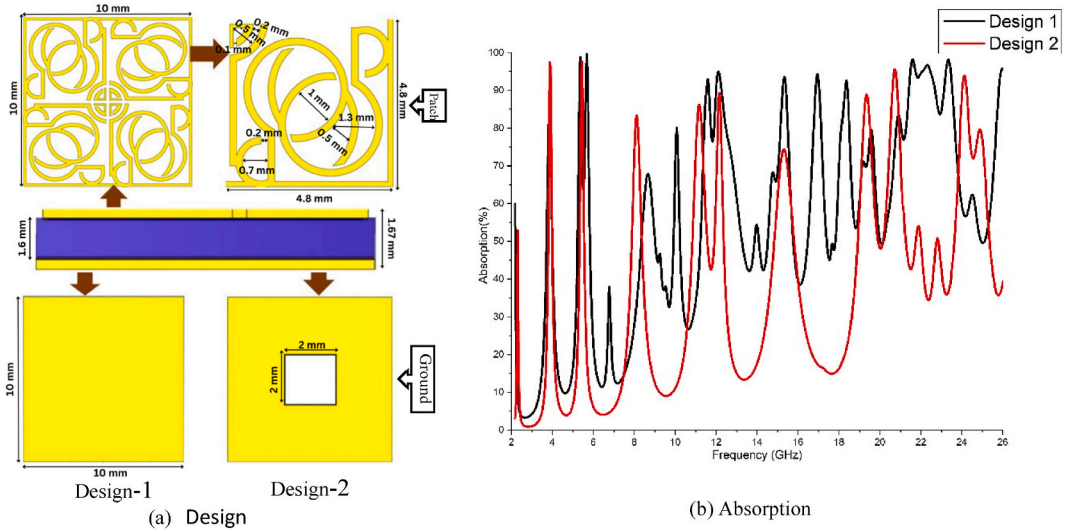

Figure-2. Polarization selective metamaterial absorber.

insensitivity. Without the border, the absorber still produced multiple resonances but with slightly reduced efficiency, especially at higher frequencies. The absence of the defined boundary led to a minor reduction in absorption performance and polarization selectivity. In the final design (Design 5), we reintroduced the square border, along with a circular shape in the centre. This combination resulted in the desired performance, with the square border and circular elements working together to enhance absorption and polarization insensitivity. This final configuration produced eight distinct resonances, with absorption rates consistently exceeding 90 %, making it highly effective for Ultra-Wideband (UWB) applications. The square border played a key role in optimizing the overall electromagnetic response, allowing for strong control over both co-polarized and cross-polarized waves. This final design proved to be the most effective, achieving wide-angle Absorption, high efficiency, and polarization insensitivity across the 2 GHz–26 GHz frequency range. This methodology introduces a pioneering design approach for achieving multiple resonance frequencies in a polarization-insensitive metamaterial absorber. The unique structural design, material selection, rigorous simulation, and experimental validation demonstrate the absorber's efficacy and hold promise for transformative advancements in absorber design and electromagnetic wave manipulation across diverse applications [10].

The distinctive design strategy employed in the proposed absorber emerges as a polarization-selective metamaterial absorber showed in Fig. 1. The introduction of a full ground layer in design-1 of Fig. 2(a) ensures exclusive co-polar Absorption, allowing the transmission of cross-polarized electromagnetic waves. This deliberate configuration provides a tailored solution for scenarios where mitigating interference from unwanted polarizations is crucial. In design-2 of Fig. 2(a), the strategic inclusion of a 2 mm square cut in the centre of the ground layer transforms the absorber into a perfect metamaterial, proficient in absorbing both co and cross-polarized electromagnetic waves. Remarkably, this polarization-selective metamaterial absorber maintains consistency in patch and substrate characteristics across both configurations, underscoring its versatility. In Fig. 2(b), the resonant data, spanning from 3.728 GHz to 22.664 GHz, further validate the absorber's efficacy, showing absorption rates exceeding 90 % at distinct resonant frequencies. This unique metamaterial design, with its polarization-selective capabilities and exceptional absorption performance, holds significant promise for applications demanding precise control over polarization states, such as in wireless communication systems, radar technologies, and electromagnetic interference shielding [11].

The patch geometry of the metamaterial absorber, specifically the Y-shaped structure, includes several blank spaces. These blank areas are not conductive, and as a result, they cause reflection rather than transmission of electromagnetic waves. When an electromagnetic wave encounters these blank spaces, the wave cannot pass through the absorber but is instead reflected. This reflection is necessary to enhance Absorption because the wave is trapped between the patch and the ground plane, allowing the resonator to absorb the energy more efficiently. These blank spaces also contribute to creating multiple resonant modes within the structure, as the distribution of surface currents is altered by the gaps in the conductive material. This helps to induce strong resonances for both co- and cross-polarized waves.

In a typical full ground plane, the design favours co-polarized Absorption, with cross-polarized waves either reflected or transmitted, leading to an imbalance in absorption efficiency. However, introducing a square cut disrupts the uniformity of the ground plane, allowing for a more balanced interaction with electromagnetic fields from both polarizations. This modification alters the boundary conditions between the patch and ground, ensuring that the absorber supports resonances equally for both co- and cross-polarized waves. By addressing this asymmetry, the square cut allows for nearly identical Absorption at the same resonance

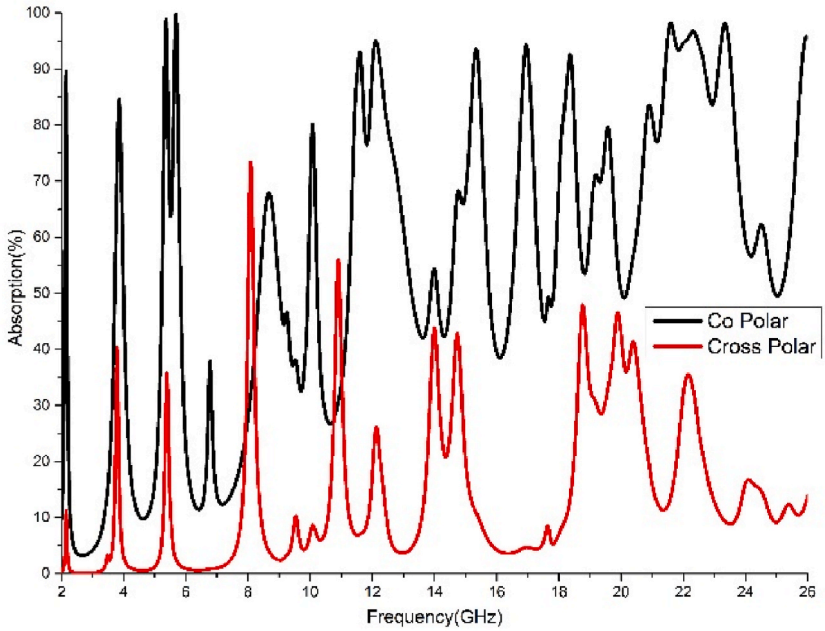

Figure-3. Co polarized & cross absorption for full ground.

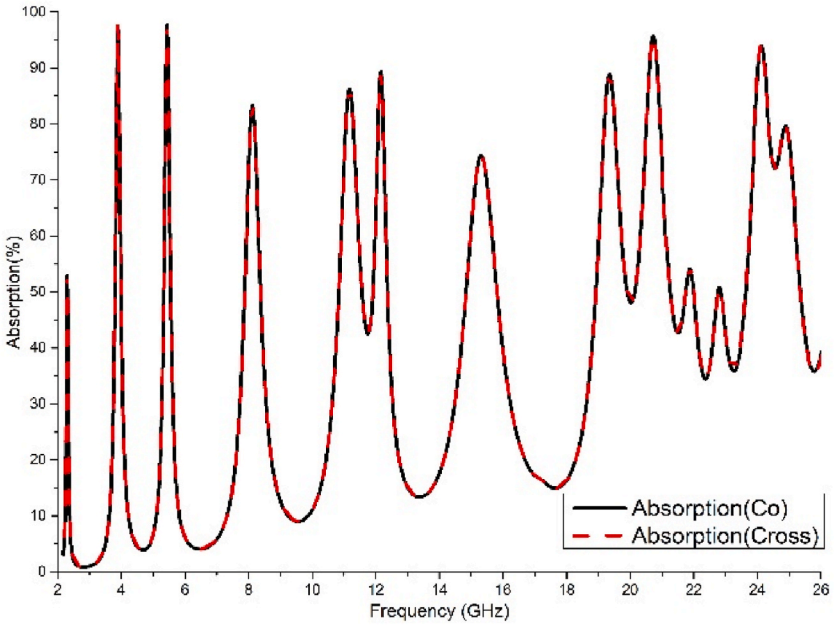

Figure-4. Co polarized & cross absorption for square cut ground.

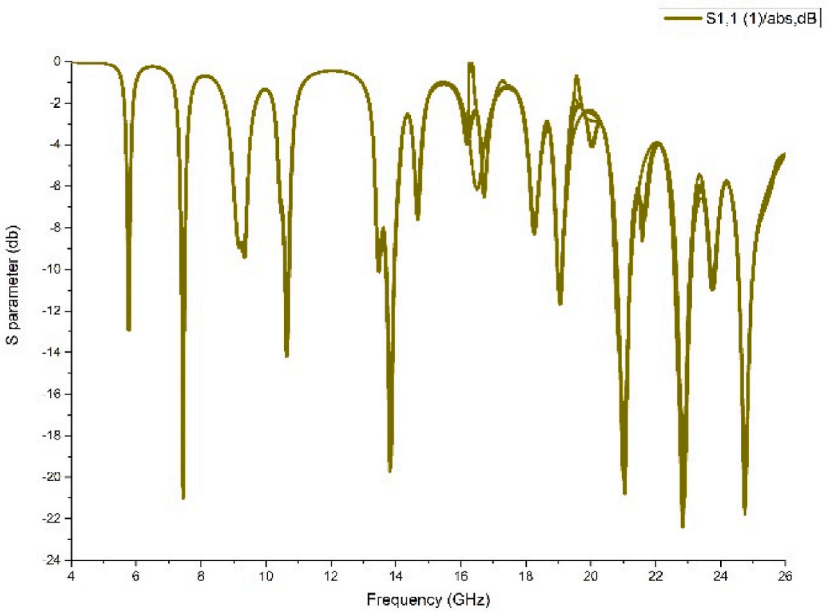

Figure-5. Scattering parameter.

frequency. The combination of the Y-shaped patch and the square cut ensures that the metamaterial absorber achieves polarization insensitivity, providing consistent and efficient Absorption for both polarizations across the same resonances.

In Fig. 3, the use of a full ground layer configuration ensures selective Absorption of co-polarized electromagnetic waves while facilitating the Absorption of cross-polarized waves. The absorption rates at 5.312 GHz, 8 GHz, 10.856 GHz, 12.056 GHz, 13.4 GHz, 20.12 GHz, and 22.664 GHz consistently exceed 90 %, emphasizing the absorber's ability to maintain high performance across a broad frequency spectrum. This design is valuable for applications requiring tailored control over polarization states, such as in wireless communication systems, where managing interference from unwanted polarizations is critical [12].

In Fig. 4, the incorporation of a 2 mm square cut in the centre of the ground layer enables the absorber to exhibit perfect Absorption for both co-polarized and cross-polarized electromagnetic waves. The patch and substrate configurations are maintained consistently

Table-1
Data at the resonance frequencies.

Operating Band	Frequency (GHz)	Absorption (%)	Permittivity	Permeability	Refractive index - DRI	Figure of Merit	Application
S-Band	3.728	98.29304	−6.00233	0	−2.76	0.15	UWB devices, wireless communication systems
C-band	5.312	91.76020	−1.60350	0	−0.52	0.03	Radar Technologies
	8	90.42	1.300256	0	1.24	0.32	Electromagnetic Interference (EMI) Shielding
X-Band	10.856	98.78220	−0.03367	0	−0.01	0.004	Microwave Imaging
	12.056	97.01479	−0.87307	0	−0.34	0.05	Aerospace and Defence
Ku-Band	13.4	99.92780	0.057792	0	0.02	0.006	Doppler Navigation Aid, satellite communications
K-Band	20.12	94.06216	1.882986	0	0.70	0.17	High-Frequency Antenna Systems
	22.664	90.51995	0.940013	0	0.29	0.07	5G Technologies

throughout the experiment. At a frequency of 3.87 GHz, the absorber achieves a high absorption rate of 97.45 %, indicating effective attenuation of incident electromagnetic waves. This trend continues at 5.44 GHz, where the absorption rate remains consistently high at 97.68 %. The absorber maintains its efficiency even at higher frequencies, with absorption rates of 95.63 % at 20.73 GHz and 93.94 % at 24.12 GHz. This design modification enhances the absorber's versatility, allowing it to effectively capture and dissipate incident waves with varying polarization states (see Fig. 5).

This metamaterial absorber configuration holds promise for applications requiring polarization-selective Absorption, offering a solution for scenarios where control over both co-polarized and cross-polarized waves is essential. The design's ability to maintain high absorption rates at various frequencies makes it suitable for applications in radar technologies, wireless communication, and electromagnetic interference mitigation [13].

3. Analysis of the metamaterial absorber

In Table 1, The provided data outlines the performance characteristics of a multi-resonance metamaterial absorber across different frequency bands, showcasing its potential applications in various technological domains. At the S-Band frequency of 3.728 GHz, the absorber exhibits exceptional absorption efficiency at 98.29 %, making it suitable for wireless communication systems. In the C-band at 5.312 GHz, with an absorption rate of 91.76 %, the absorber proves valuable for radar technologies. At 8 GHz, the absorber achieves an absorption rate of 90.42 %, positioning it as an effective solution for Electromagnetic Interference (EMI) shielding applications. Transitioning to higher frequencies, the X-Band (10.856 GHz) and Ku-Band (13.4 GHz) demonstrate absorption rates of 98.78 % and 99.93 %, respectively, suggesting applications in microwave imaging and satellite communications. The absorber's efficacy extends to the K-Band (20.12 GHz) with a 94.06 % absorption rate, indicating suitability for high-frequency antenna systems, while the 22.664

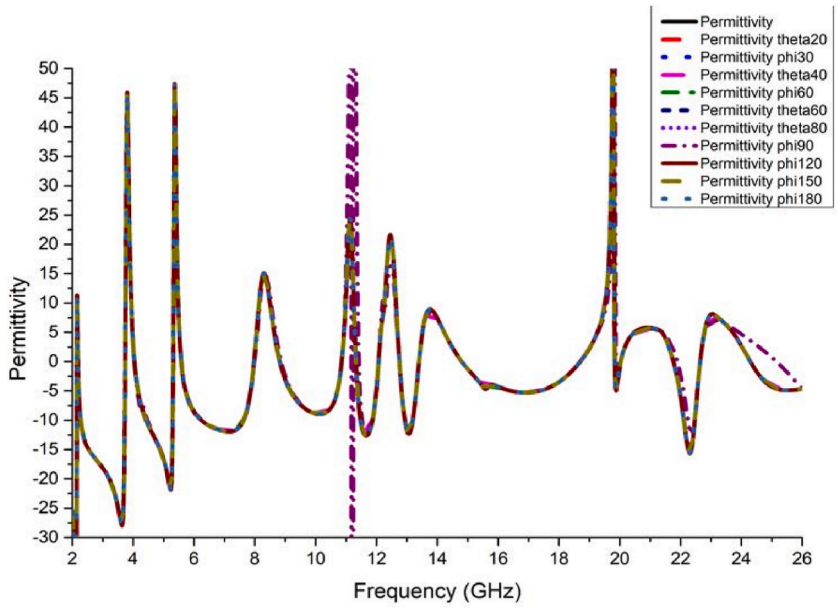

Figure-6. Permittivity.

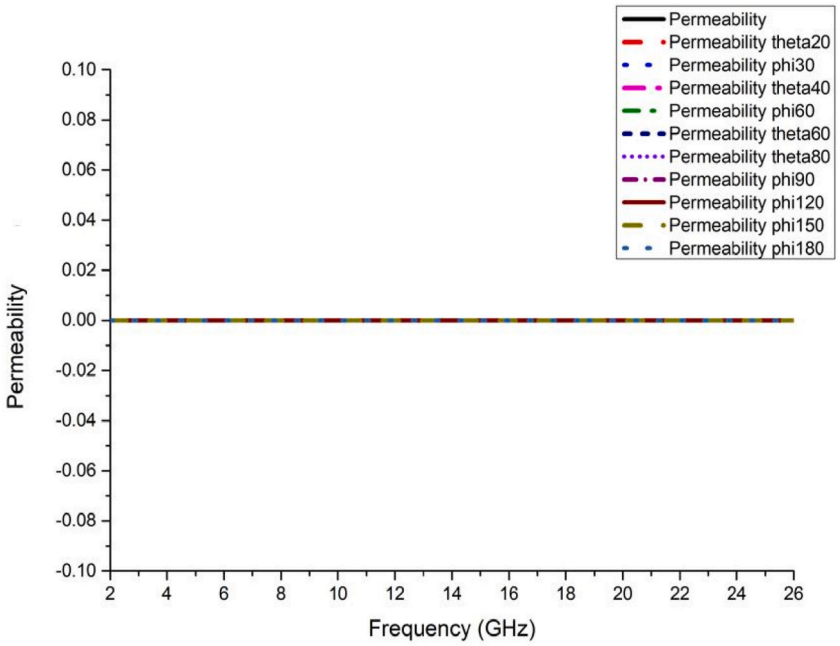

Figure-7. Permeability.

GHz frequency shows promise for 5G technologies with a 90.52 % absorption rate. The provided data underscores the versatile applications of the metamaterial absorber across a wide range of frequency bands, catering to the needs of diverse technological fields.

The Y-shaped SRR structure consists of several important elements: the copper patches, the dielectric FR-4 substrate, and the square cut introduced in the ground plane. These components interact to create a highly resonant system. The Y-shaped structure behaves similarly to an inductive loop, where circulating currents produce magnetic dipole moments in response to the incident magnetic field. These magnetic dipole moments directly contribute to the material's effective permeability. In traditional SRR structures, the rings or split rings create localized magnetic fields that induce currents, leading to a magnetic response at specific frequencies. However, the bent Y-shaped geometry breaks the conventional magnetic symmetry, which weakens the magnetic response across the entire frequency range. The modified geometry disrupts the usual inductive behaviour, thus forcing the structure into a zero magnetic response across the operating bands (see Fig. 6).

In Fig. 10, The surface current distributions observed in simulations further explain this phenomenon. At resonant frequencies, the currents are primarily concentrated along the edges of the Y-shaped structure, but the geometry causes these currents to cancel each other out, preventing the formation of significant magnetic dipoles. This behaviour leads to a vanishing effective magnetic response, thus driving the permeability close to zero across all bands. In this specific design, the near-zero permeability is an intended feature to achieve perfect Absorption across the broadband. By suppressing magnetic resonance through the geometry of the Y-shaped SRR, the structure essentially eliminates magnetic dipole formation at any of the resonant frequencies. As a result, the magnetic response is minimized, leading to zero permeability ($\mu r \approx 0$) across the entire frequency range, as verified in Fig. 7 of the manuscript. By eliminating magnetic resonance, the structure prevents the reflection and transmission of waves, thereby enhancing Absorption across a wide frequency range. The zero-permeability characteristic ensures that the metamaterial can maintain high absorption efficiency over multiple bands, as evidenced by the eight resonant frequencies described in the manuscript (3.728 GHz–22.664 GHz) (see Fig. 8).

The metamaterial absorber exhibits exceptional absorption characteristics across diverse microwave frequencies, showing absorption rates ranging from approximately 90 % to nearly 99.93 %. This remarkable efficiency in attenuating incident electromagnetic waves highlights the absorber's capability to interact selectively with electromagnetic fields across the frequency spectrum. At distinct resonant frequencies, particularly at 13.4 GHz and 3.728 GHz, the absorber demonstrates outstanding absorption performance. These resonant frequencies correspond to the specific design and geometry of the metamaterial structure, allowing for strong electromagnetic coupling and resonance effects at these points.

The absorber's absorption efficiency is intricately linked to its unique permittivity and permeability characteristics showed in Figs. 6 and 7. These material properties dictate the absorber's interaction with incident electromagnetic waves, facilitating effective

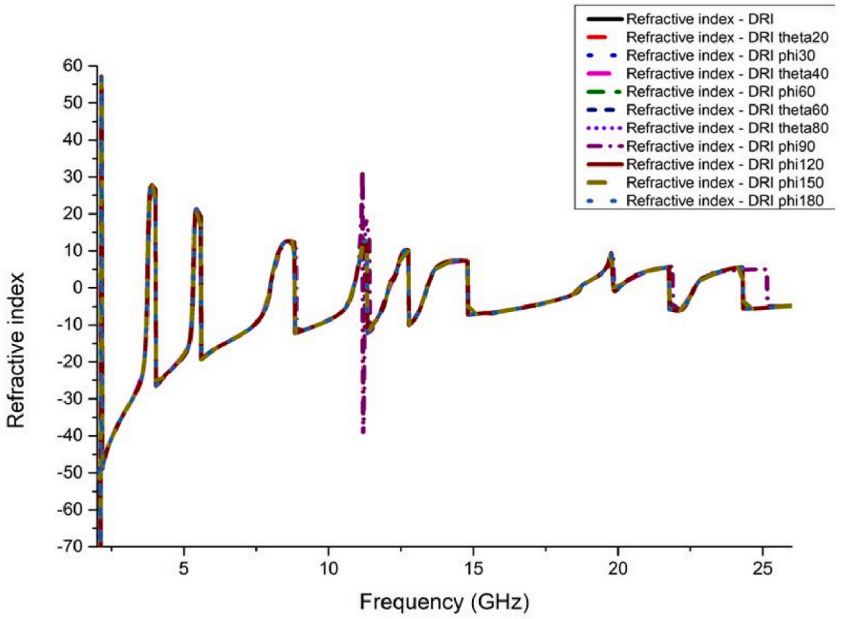

Figure-8. Refractive index.

Absorption by matching the impedance and maximizing energy dissipation at resonant frequencies. Resonant frequencies exhibiting superior absorption rates, such as 13.4 GHz and 3.728 GHz, hold significant potential for targeted applications. Their precise absorption behaviour enables tailored usage in radar technologies, wireless communication systems, and scenarios demanding precise electromagnetic interference control [14].

To assess incident angle insensitivity, systematically varied the incident angles (θ) from 0 to 80° and azimuthal angles (ϕ) from 0 to 180° in increments. The absorber's performance was consistently monitored across these variations. The absorption results remained invariant, emphasizing the robust incident angle insensitivity of the metamaterial design. The simulation results revealed that altering the incident and azimuthal angles had negligible effects on the absorber's absorption performance showed in Fig. 9. Absorption rates exceeding 90 % were consistently observed, signifying the absorber's ability to efficiently capture and dissipate incident electromagnetic waves, regardless of their polarization orientation [15].

The simulations were conducted for both Transverse Electric (TE) and Transverse Magnetic (TM) modes. The results indicate that the absorber maintains high absorption rates (above 90 %) for incident angles up to 80° for theta and 180° for phi for both modes. The design's polarization-selective nature ensures efficient wave absorption across both TE and TM modes, making it highly versatile for various environmental conditions. Additionally, the manuscript has been enhanced to include a more detailed explanation of the simulation setup for angle variation, demonstrating how the absorber performs under different angles of incidence.

Across the resonant bands, the surface currents exhibit intricate variations, influencing the absorption efficiency of the metamaterial absorber [16]. The resonant frequencies, including notable peaks at 3.728 GHz and 13.4 GHz, showcase unique surface

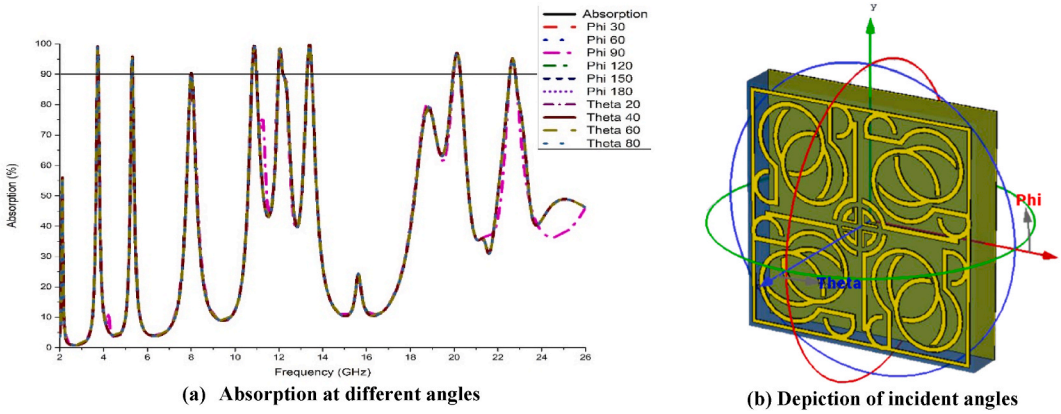

(a) Absorption at different angles (b) Depiction of incident angles

Figure-9. Incident angle insensitivity of the absorber.

current dynamics, emphasizing the absorber's tailored response to incident waves. The observed surface current patterns offer valuable insights into the absorption mechanisms at play in the metamaterial absorber. The resonance-induced surface currents contribute significantly to the absorber's ability to capture and dissipate incident electromagnetic waves effectively. The discussion delves into the implications of these surface current dynamics on the absorber's performance and its suitability for diverse applications [17].

This paper shows distinct patterns of E-field and H-field distribution at each resonant frequency showed in Fig. 11 and Fig. 12. Across the resonant bands, the electromagnetic fields exhibit intricate variations, showing the absorber's tailored response to incident waves. The resonant frequencies, including notable peaks at 3.728 GHz and 13.4 GHz, demonstrate unique E-field and H-field dynamics, emphasizing the absorber's ability to selectively interact with incident electromagnetic waves. The observed E-field and H-field patterns offer valuable insights into the absorption mechanisms at play in the metamaterial absorber. The resonance-induced electromagnetic field responses contribute significantly to the absorber's efficiency in capturing and dissipating incident electromagnetic waves. The discussion delves into the implications of these field dynamics on the absorber's performance and its suitability for diverse applications [18].

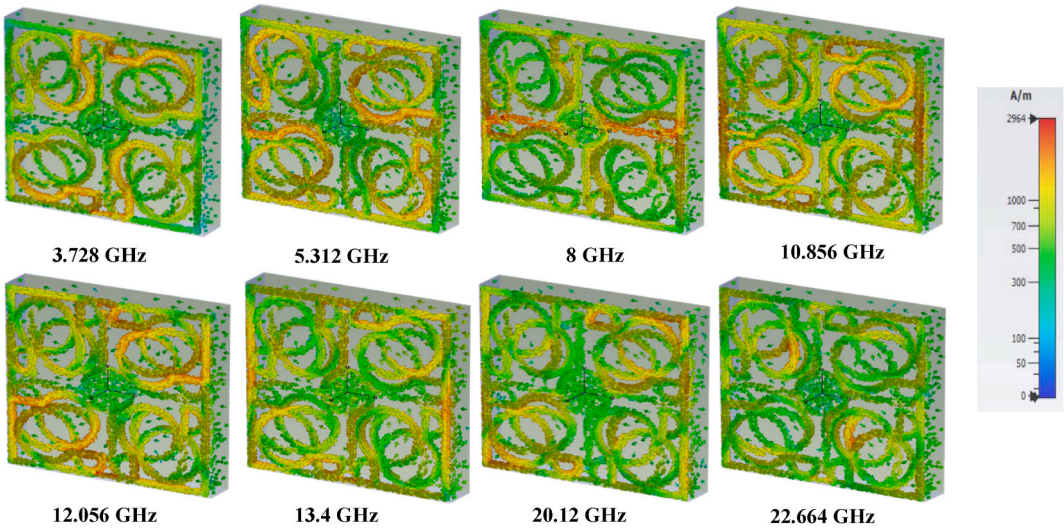

Figure-10. Surface current distributions at the resonance frequencies.

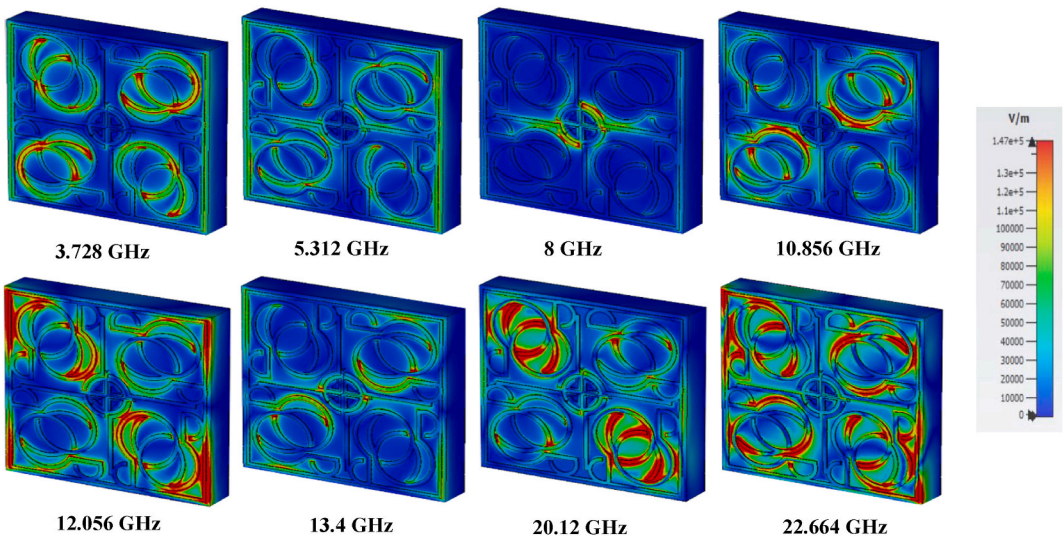

Figure-11. Electric Field distributions at the resonance frequencies.

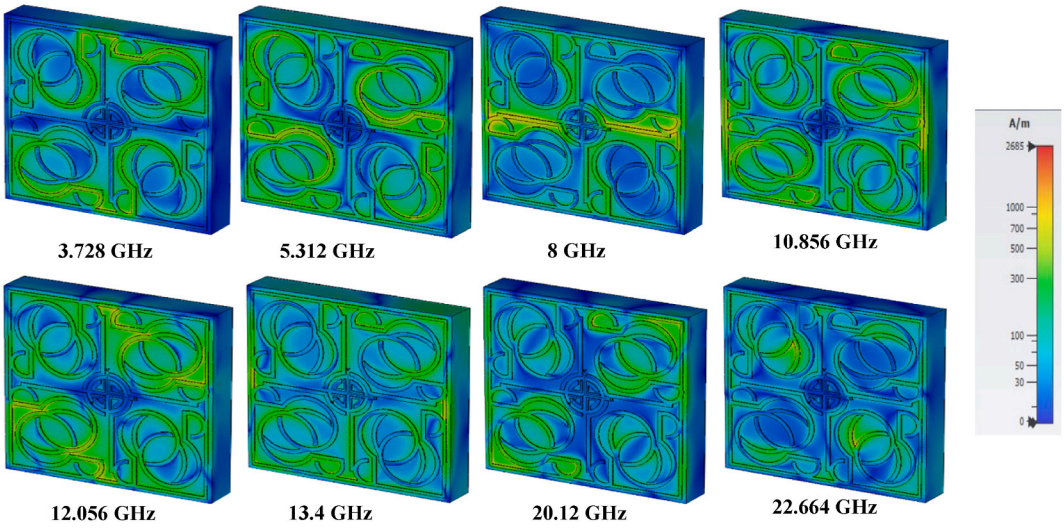

Figure-12. Magnetic Field distributions at the resonance frequencies.

4. Equivalent circuit of the proposed absorber

While designing a metamaterial absorber, inductance (L), capacitance (C), and resistance (R) come together to provide resonance by trapping EM waves in particular frequencies [19]. Here in our proposed design, this inductance is working for copper annealed, and the absorber patch is not solid as lots of cuts are present on the patch, and there is a dielectric gap in between the patch and ground because of the FR-4, which are working as capacitance, and while the charge is flow through the inductive element that also hold some default resistance. Here, in Fig. 13, each RLC circuit is responsible for a particular reflection coefficient that provides a value under −10dB. Still, all RLC circuits are working in a cluster to show the results we got because all resonances are from one particular patch. A different portion of the patch works for different resonances, where those points that are not working for a particular resonance work as catalysts. Come into the circuit, the terms G2 and G1 define the free space EM ports where the impedance is 377 Ω.

All the values that we mentioned in the circuit are calculated by observing the surface current produced for the resonance frequencies in all points, where we used the length (l) and width (w) of the inductive portions of the patch, which further used in equations (5) and (6) to find inductance and capacitance [20].

$$L_{ims} = 0.00508l\left[\ln\left(\frac{2l}{w+h}\right) + 0.5 + 0.2235\ \frac{(w+h)}{l}\right] \tag{5}$$

Here, in equation 5, l and w define the length and width of the inductive portion, which changed according to the resonances, and h

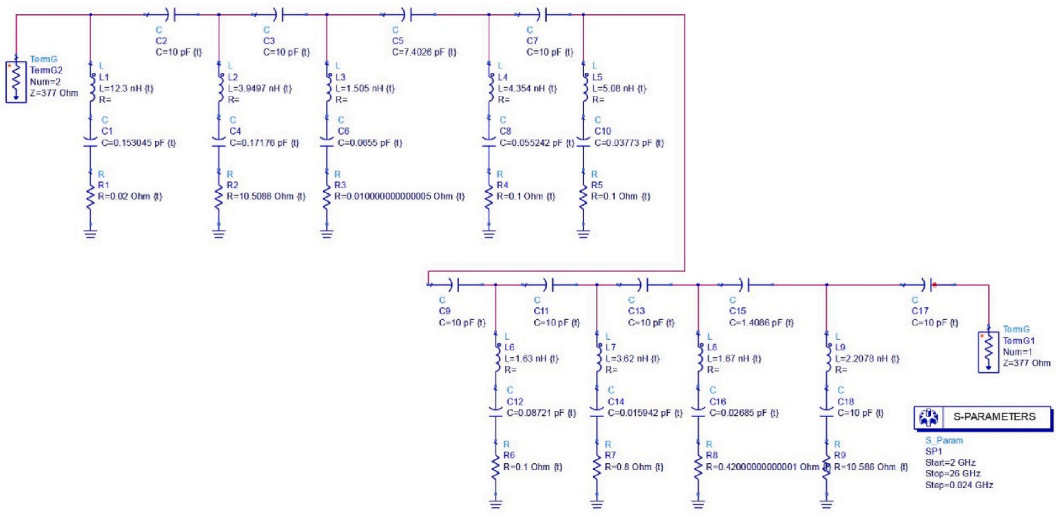

Figure-13. Simplified equivalent circuit of the absorber.

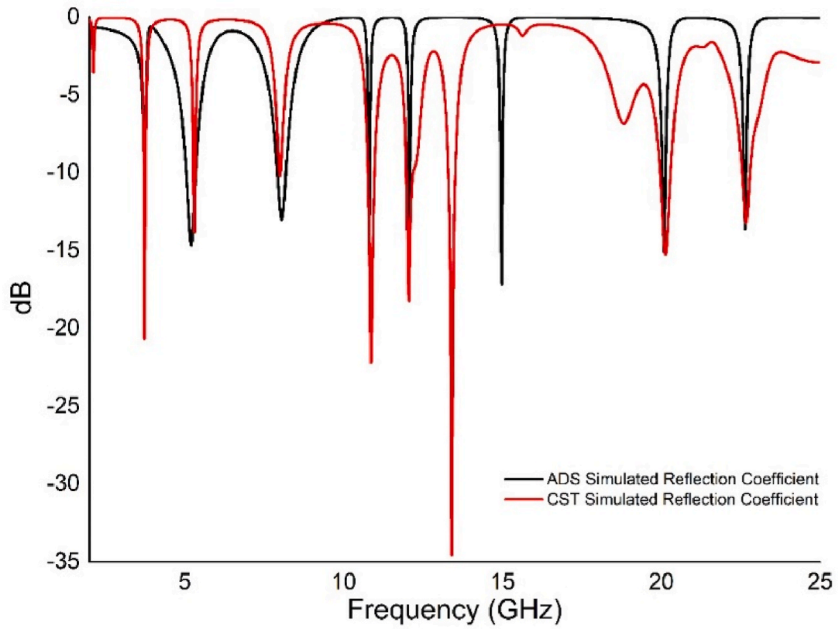

Figure-14. Comparison of the S parameter in CST and ADS Circuit Simulator.

is the distance between the patch and the ground. L_{ims} is the inductance that will further put on equation (6) to find the capacitance C, where f is the specific frequency for which we obtain capacitance and inductance [21].

$$2\pi f = \frac{1}{\sqrt{l_{ims}C}} \tag{6}$$

From Fig. 14, we can observe that we get results that are nearly similar to those we got from the CST simulation, but we also see a shift of resonance frequency from 13.4 GHz, which is because of the resonances we worked on while designing the ads circuit. When we

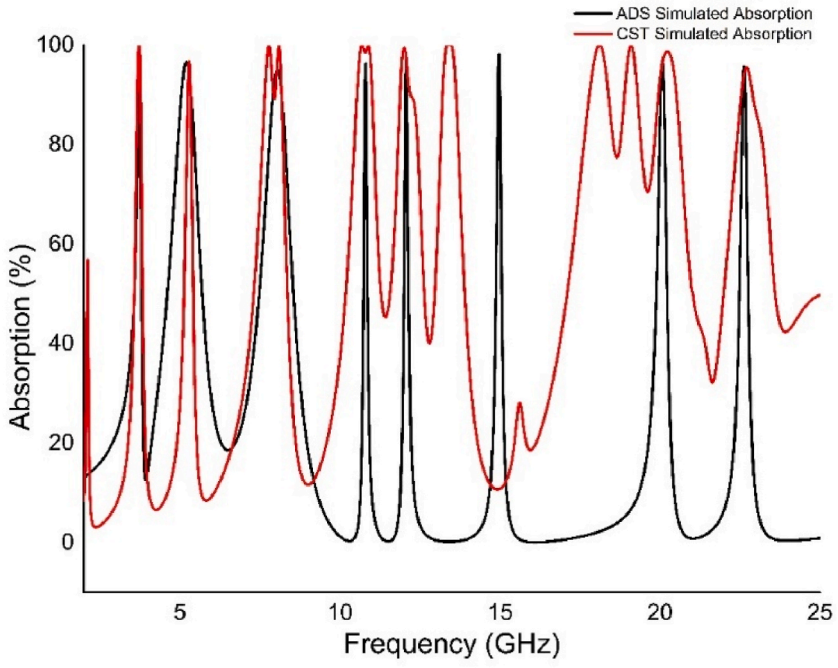

Fig. 15. Comparison of the absorption in CST and ADS Circuit Simulator.

design an ADS circuit, we integrate all RLC values whose reflection coefficient is under −10dB. That's why this slightly affects the results, as other portions of the patch, which are not directly involved in resonance, work as a catalyst. This is also the main reason why, in Fig. 15, we got some extra absorption peaks and shifts in the result of Absorption, but we didn't count that, as their reflection coefficient is not under −10dB [22].

5. Measurement of the proposed absorber

In Fig. 16, the absorber was fabricated with 10 × 10 (mm) dimensions to optimize electromagnetic Absorption, featuring an array of Y-shaped structures on an FR-4 substrate, which enhanced its performance across multiple frequency bands. The absorber array's layout was designed to maximize surface current distribution and resonance behaviour, while the material choice of copper patches supported efficient Absorption. For the measurement setup, the absorber was positioned between waveguide ports, and reflection (S11) and transmission (S21) coefficients were measured using a Vector Network Analyzer (VNA). Multiple waveguide port configurations were used to test different resonance frequency ranges, ensuring thorough data collection. The reflection and transmission coefficients were analysed to calculate Absorption, following equation (1).

In Fig. 17, the measured results show that the absorber achieved high absorption rates at its main resonance frequencies. At 3.728 GHz, the Absorption reached 98.29 %, while at 5.312 GHz, it recorded 91.76 %. Additionally, the absorber exhibited 90.42 % absorption at 8 GHz and an impressive 98.78 % at 10.856 GHz. The resonance frequency at 12.056 GHz showed a strong absorption rate of 97.01 %. Furthermore, the absorber demonstrated excellent performance at higher frequencies, with 99.93 % absorption at 13.4 GHz, 94.06 % at 20.12 GHz, and 90.52 % at 22.664 GHz. These resonance points exhibited excellent absorption efficiency, closely

(a) (b)

Fig. 16. Measurement of the Proposed Absorber (a) With VNA and Waveguide Ports, (b) unit cell.

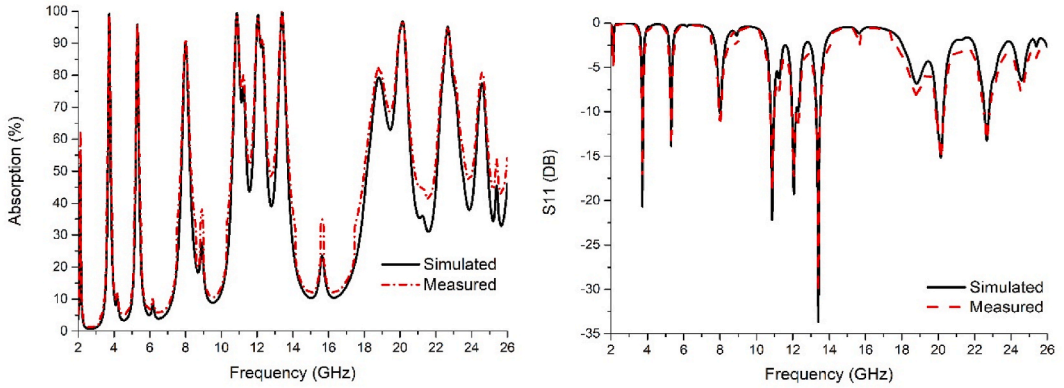

(a) (b)

Fig. 17. Comparison between (a) measured absorptions and simulated absorptions and (b) measured reflection coefficient with simulated results.

matching the simulated results. The S11 parameter measurements across these frequencies consistently showed reflection coefficients below −10 dB at resonance, demonstrating the absorber's effectiveness in minimizing reflections and maximizing energy dissipation. This characteristic ensures the absorber's practical relevance in applications where minimizing reflection and maximizing Absorption are crucial. The measured data, including these key resonance frequencies and absorption percentages, confirm the absorber's high absorption efficiency, making it suitable for ultra-wideband (UWB) devices and Doppler navigation systems. The close alignment with simulations validates the absorber's potential for real-world applications.

6. Discussion

The presented metamaterial absorber design, incorporating a 2 mm square cut in the centre of the ground layer, has been systematically analysed and tested across a range of frequencies to evaluate its effectiveness in achieving selective polarization absorption [23,24]. The investigation into the equivalent circuit parameters of the proposed metamaterial absorber design unveils crucial insights into its resonance behaviour and absorption characteristics. By considering inductance, capacitance, and resistance, we gain a comprehensive understanding of the underlying electromagnetic interactions driving absorption efficiency. The ability of the metamaterial absorber to operate efficiently within the UWB frequency range highlights its suitability for modern communication systems. By achieving high absorption rates and minimizing interference, the absorber can significantly enhance UWB device performance, leading to more reliable and efficient communication. This highly efficient MMA also demonstrates its potential application in Doppler navigation aids, providing accurate and reliable navigation data essential for aviation and maritime navigation. The absorber exhibits remarkable absorption characteristics for both co-polarized and cross-polarized electromagnetic waves, validating its potential for diverse applications [25,26].

The novelty of our work lies in the tailored Y-shaped Split Ring Resonator (SRR) design, which is uniquely optimized for polarization-selective Absorption across a wideband spectrum, from 2 GHz to 26 GHz. This design shows eight distinct resonances with absorption rates exceeding 90 % at each frequency. The polarization insensitivity coupled with near-zero permeability is a significant innovation, as this combination has not been widely explored for such a broad frequency range. In the revised manuscript, we explicitly discuss how this frequency range covers multiple communication and radar bands, emphasizing its novel contributions to UWB device applications, Doppler navigation aids, and EMI shielding technologies. Analysing the frequency-specific absorption rates, it is evident that the absorber consistently achieves high absorption percentages. At 3.87468 GHz and 5.43576 GHz, the absorber demonstrates absorption rates of 97.45 % and 97.68 %, respectively. Even at higher frequencies, such as 20.73434 GHz and 24.12069 GHz, the absorber maintains efficiency with absorption rates of 95.63 % and 93.94 %. This trend underscores the absorber's versatility in providing reliable Absorption across a spectrum of frequencies.

Here, the frequency range of 2 GHz–26 GHz was selected for its optimal balance between data rate, bandwidth, and signal propagation characteristics. This range allows for higher bandwidths, which are essential for supporting the high data rates required in modern applications such as 5G communications and high-speed internet. Additionally, this spectrum offers multiple channels, enabling a greater number of users while minimizing interference. Frequencies at the lower end of the spectrum, around 2 GHz, provide better penetration through obstacles and longer-range capabilities, making them suitable for applications requiring broad coverage, such as cellular networks. In contrast, the higher frequencies, extending up to 26 GHz, offer increased resolution and capacity, making them ideal for high-definition imaging and radar systems. However, it is important to note that these higher frequencies

Table-2
Comparison of the proposed absorber with the relevant work.

Ref no	Year	Resonance Frequency (GHz)	Substrate Material	Dimension	Maximum Absorption	EMR	Maximum angle of Absorption for		Co and Cross polar Absorption	SNG/ DNG
							Theta	Phi		
[27]	2023	4.6, 6.44, 7.89 and 12.44,	FR-4	0.14λ × 0.14λ	99 %	5.43	60°	60°	Co & Cross	N/M
[28]	2023	27.09, 38.71, and 41.81	Rogers RT5880	0.45λ × 0.45λ	N/M	2.21	35°	35°	Co	SNG
[29]	2023	9.90, 10.21. 10.05	FR-4	0.78λ × 0.35λ	N/M	N/M	N/M	N/M	Co	N/M
[30]	2024	4.46, 11.48	FR-4, RO-3035, RO-5880, and RO-6202	0.215λ × 0.215λ	N/M	4.64	N/M	N/M	Co & Cross	SNG
[31]	2023	3.2, 5.4	Rogers RT 5880	0.106λ × 0.106λ	99.98 %	9.37	45°	90°	Co and Cross	SNG
Proposed	2024	3.728, 5.312, 8, 10.856, 12.056, 13.4, 20.12, 22.664	FR-4	0.124λ × 0.124λ	99.9 %	8.05	80°	180°	Polarization Selective (Co or Co &cross)	SNG

come with challenges, such as a reduced range and greater sensitivity to obstacles and adverse weather conditions. Thus, the chosen frequency range effectively addresses the diverse needs of contemporary communication and imaging technologies, optimizing performance across various applications.

In Table 2, The proposed absorber covers a broad range of frequencies, including 3.728 GHz, 5.312 GHz, 8 GHz, 10.856 GHz, 12.056 GHz, 13.4 GHz, 20.12 GHz, and 22.664 GHz, providing versatility across different applications. With a remarkable 99.9 % maximum absorption, it outperforms many others, indicating superior efficiency in attenuating incident electromagnetic waves. This metamaterial absorber stands out with a notably high EMR value of 8.05, indicating its superior effectiveness in simulating the desired effective medium compared to other absorbers in the comparison. This high EMR value suggests that the proposed absorber achieves an exceptional level of emulation, closely approximating the electromagnetic response of the desired effective medium. Also, it Demonstrates Absorption at a maximum angle of 80° for theta and 180° for phi, showing adaptability to incident waves arriving from various directions. The proposed absorber is designed for polarization-selective (co/co &cross) absorption, offering flexibility for both co-polar and cross-polar absorptions and enhancing its adaptability to diverse scenarios [32–34]. The proposed absorber operates as a Single-Negative (SNG) metamaterial, aligning with contemporary design preferences for efficient Absorption. These characteristics position it as a promising candidate for applications demanding high-performance metamaterial absorbers [35,36].

7. Conclusion

In this paper, we introduced a novel type of metamaterial absorber designed using a Y-shaped Split Ring Resonator (SRR) structure. Our design stands out for its exceptional performance in absorbing electromagnetic waves across a broad frequency range from 2 GHz to 26 GHz. This wide bandwidth includes several key frequency bands, such as the L, S, C, X, Ku, and K bands, which are critical for various technological applications. The absorber features eight distinct resonant frequencies where it achieves absorption rates exceeding 90 %. This high level of Absorption across such a broad range makes it highly suitable for applications that require wide-bandwidth Absorption, such as Ultra-Wideband (UWB) devices, Doppler navigation aids, and electromagnetic interference (EMI) shielding. The ability to absorb a wide range of frequencies efficiently is crucial for these applications, as it ensures that the device can handle a variety of signal types and frequencies effectively. One of the notable advancements of our design is its polarization insensitivity. This feature is achieved through a unique modification: a square-shaped cut in the centre of the ground plane. This design allows the absorber to perform effectively with both co-polarized and cross-polarized waves. This polarization insensitivity is particularly beneficial in real-world scenarios where the polarization of incoming signals may vary, making the absorber versatile and reliable across different environments. Additionally, our absorber maintains high absorption rates even when the incident waves strike it at angles up to 80°. This ability to perform well at various angles enhances its practical utility, as it can effectively absorb waves that come from different directions, a common situation in many practical applications.

A significant feature of our design is its near-zero permeability throughout the entire frequency range. This characteristic represents a major step forward in metamaterial design, as it allows for highly efficient absorption of electromagnetic waves. By overcoming the limitations of traditional absorbers, our design sets a new standard for performance in this field. Although the results presented in this paper are based on simulation data, the next steps will involve fabricating a physical version of the absorber and conducting experimental tests to validate its practical effectiveness. This future work will help confirm the design's real-world performance and open up opportunities for developing advanced metamaterial absorbers. Such absorbers could have a wide range of applications, including telecommunications, radar technologies, and other systems that manage electromagnetic waves, potentially leading to significant advancements in these fields.

CRediT authorship contribution statement

Sayed Mahmud: Writing – review & editing, Writing – original draft, Visualization, Validation, Software, Resources, Methodology, Investigation, Data curation, Conceptualization. **Apurba Ray Chowdhury:** Writing – review & editing, Validation, Methodology, Formal analysis. **Saif Hannan:** Writing – review & editing, Supervision, Investigation. **Mohammad Tariqul Islam:** Funding acquisition. **Ahmed S. Alshammari:** Funding acquisition. **Mohamed S. Soliman:** Funding acquisition.

Data availability statement

Data will be made available on request to the corresponding author.

Funding

This work was supported by the Ministry of Higher Education (MOHE), Malaysia, through the Fundamental Research Grant Schemes (FRGS) under Grant FRGS/1/2021/TK0/UKM/02/30.

Declaration of competing interest

The authors confirm that there are no known financial or personal conflicts that could have influenced the findings presented in this paper.

References

[1] N.I. Landy, S. Sajuyigbe, J.J. Mock, D.R. Smith, W.J. Padilla, Perfect metamaterial absorber, Phys. Rev. Lett. 100 (20) (May 2008), https://doi.org/10.1103/PhysRevLett.100.207402.

[2] F. Verde, V. Galdi, L. Zhang, T.J. Cui, Integrating sensing and communications: simultaneously transmitting and reflecting digital coding metasurfaces [Online]. Available: http://arxiv.org/abs/2406.10826, Jun. 2024.

[3] Y. Wang, et al., Split ring hole metamaterial-enhanced pyroelectric detector for efficient multi-narrowband terahertz detection, Opt Express 32 (11) (May 2024) 19779, https://doi.org/10.1364/oe.522788.

[4] I.M.T. Islam, S.S. Islam, Md R. Islam, A.N. Md R. Karim, R. Azim, Nano-structured metamaterial absorber based on a plus-shaped resonator for optical wavelength applications, J. Eng. Appl. Sci. 71 (1) (Dec. 2024) 134, https://doi.org/10.1186/s44147-024-00465-z.

[5] A.R. Chowdhury, S. Hannan, M.K. Uddin, M.E.H. Bhuiyan, M.I. Hoque, M.T. Islam, Gas stove burner shape with inductive tailed rotational symmetric metamaterial absorber for C and X band application, in: 2023 International Conference on Next-Generation Computing, IoT and Machine Learning (NCIM), 2023, pp. 1–5, https://doi.org/10.1109/NCIM59001.2023.10212988.

[6] S. Hannan, et al., A filling-factor engineered, perfect metamaterial absorber for multiple applications at frequencies set by IEEE in C and X bands, J. Mater. Res. Technol. 19 (Jul. 2022) 934–946, https://doi.org/10.1016/j.jmrt.2022.05.071.

[7] M. Berka, et al., A miniaturized folded square split ring resonator cell based dual band polarization insensitive metamaterial absorber for C- and Ku-band applications, Opt Quantum Electron 55 (8) (Aug. 2023), https://doi.org/10.1007/s11082-023-04954-y.

[8] H. Pang, et al., Research advances in composition, structure and mechanisms of microwave absorbing materials, Compos. B Eng. 224 (2021) 109173, https://doi.org/10.1016/j.compositesb.2021.109173.

[9] J. Zhou, et al., Metamaterial and nanomaterial electromagnetic wave absorbers: structures, properties and applications, J Mater Chem C Mater 8 (37) (2020) 12768–12794.

[10] M.Q. Dinh, T. Le Hoang, H.T. Vu, N.T. Tung, M.T. Le, Design, fabrication, and characterization of an electromagnetic harvester using polarization-insensitive metamaterial absorbers, J. Phys. D Appl. Phys. 54 (34) (2021) 345502.

[11] Y.I. Abdulkarim, et al., A review on metamaterial absorbers: microwave to optical, Front Phys 10 (2022) 893791.

[12] Assessment on use of spectrum in the 10-17 GHz band for the GSO fixed-satellite service in Region 1 S Series Fixed satellite service" [Online]. Available: http://www.itu.int/ITU-R/go/patents/en.

[13] H. Yu, P. Li, J. Su, Z. Li, S. Xu, F. Yang, Reconfigurable bidirectional beam-steering aperture with transmitarray, reflectarray, and transmit-reflect-array modes switching, IEEE Trans. Antenn. Propag. 71 (1) (2023) 581–595, https://doi.org/10.1109/TAP.2022.3222337.

[14] M.C. Tran, et al., Controlled defect based ultra broadband full-sized metamaterial absorber, Sci. Rep. 8 (1) (Dec. 2018), https://doi.org/10.1038/s41598-018-27920-1.

[15] M. Kim, K. Jung, Y. Choi, S.S. Hwang, J.K. Hyun, Coupled solid and inverse antenna stacks above metal ground as metamaterial perfect electromagnetic wave absorbers with extreme subwavelength thicknesses, Adv. Opt. Mater. 10 (10) (2022) 2101672.

[16] W. Li, M. Xu, H.-X. Xu, X. Wang, W. Huang, Metamaterial absorbers: from tunable surface to structural transformation, Adv. Mater. 34 (38) (2022) 2202509.

[17] S.M. Sijan, S. Hannan, O. Faruk, Md Ibrahim, Md A. Hossain, Eye-shaped labyrinth metamaterial absorber for C, X, Ku & K-band applications, in: 2023 IEEE International Conference on Telecommunications and Photonics (ICTP), 2023, pp. 1–5, https://doi.org/10.1109/ICTP60248.2023.10491066.

[18] S. Banerjee, B.P. Pal, D. Roy Chowdhury, Resonance phenomena in electromagnetic metamaterials for the terahertz domain: a review, J. Electromagn. Waves Appl. 34 (10) (2020) 1314–1337.

[19] M. Raihan, et al., Octagonal enclosed octagonal-shaped metamaterial absorber based on SiO2 for the infrared region, in: International Conference on Space Science and Communication, 2023, pp. 165–174.

[20] A.R. Chowdhury, S. Hannan, M.T. Islam, S. Alamri, A.S. Alshammari, M.S. Soliman, Maze-enclosed quad symmetric kite shaped SRR based metamaterial absorber for Doppler navigation aids and earth exploration satellite remote sensing services, Alex. Eng. J. 100 (Aug. 2024) 357–368, https://doi.org/10.1016/j.aej.2024.05.034.

[21] M.I. Hoque, N. Alam, M.K. Uddin, S. Hannan, N.M. Sahar, A. Hoque, Labyrinth maze-shaped split ring EM metamaterial absorber for C and X band application, in: International Conference on Space Science and Communication, 2023, pp. 155–164.

[22] N. Misran, S.H. Yusop, M.T. Islam, M.Y. Ismail, Analysis of parameterization substrate thickness and permittivity for concentric split ring square reflectarray element, Jurnal Kejuruteraan 23 (2012) 11–16.

[23] S.B. Reddy, B. V, A comprehensive review on the characterization of nanomaterials for the suppression of electromagnetic interference across diverse frequency bands, Polymer-Plastics Technology and Materials (2024) 1–42.

[24] O.S. Lateef, M. Al-Badri, K.S.L. Al-badri, et al., Polarization-insensitive Archimedes'-spiral-shaped ultrathin metamaterial absorbers for microwave sensing application, Sci. Rep. 13 (2023) 19445, https://doi.org/10.1038/s41598-023-46363-x.

[25] M.G. Rabbani, M.T. Islam, M. Moniruzzaman, et al., Dumbbell shaped structure loaded modified circular ring resonator based perfect metamaterial absorber for S, X and Ku band microwave sensing applications, Sci. Rep. 14 (2024) 5588, https://doi.org/10.1038/s41598-024-56251-7.

[26] Elakkiya, A. Mohanan, M. Aran Thomas, R. Syed Rayaan Ahmedh, 6 Bands microwave metamaterial absorber for S, C, X, and Ku band applications, Mater Today Proc (2023), https://doi.org/10.1016/j.matpr.2023.05.636.

[27] M.B. Hossain, M.R.I. Faruque, M.T. Islam, Double elliptical resonator based quadruple band metamaterial absorber for EMI shielding applications in microwave regime, Alex. Eng. J. 69 (Apr. 2023) 193–206, https://doi.org/10.1016/j.aej.2023.01.035.

[28] M. Lutful Hakim, et al., Interconnected square splits ring resonator based single negative metamaterial for 5G (N258, N257, N260 and N259) band sensor/EMI shielding/and antenna applications, Alex. Eng. J. 81 (Oct. 2023) 419–436, https://doi.org/10.1016/j.aej.2023.09.044.

[29] M. Rashedul Islam, et al., Star enclosed circle split ring resonator-based metamaterial sensor for fuel and oil adulteration detection, Alex. Eng. J. 67 (Mar. 2023) 547–563, https://doi.org/10.1016/j.aej.2023.01.001.

[30] M.Z.B. Chowdhury, M.T. Islam, A. Alzamil, M.S. Soliman, M. Samsuzzaman, A tunable star-shaped highly sensitive microwave sensor for solid and liquid sensing, Alex. Eng. J. 86 (Jan. 2024) 644–662, https://doi.org/10.1016/j.aej.2023.12.001.

[31] N. Ullah, et al., An efficient, compact, wide-angle, wide-band, and polarization-insensitive metamaterial electromagnetic energy harvester, Alex. Eng. J. 82 (Nov. 2023) 377–388, https://doi.org/10.1016/j.aej.2023.10.015.

[32] N. Suresh Kumar, K.C.B. Naidu, P. Banerjee, T. Anil Babu, B. Venkata Shiva Reddy, A review on metamaterials for device applications, Crystals 11 (5) (2021) 518.

[33] F. Zhou, et al., An ultra-broadband microwave absorber based on hybrid structure of stereo metamaterial and planar metasurface for the S, C, X and Ku bands, Results Phys. 30 (2021) 104811.

[34] Pavan Kumar, Neelesh Kumar Gupta, Achyuta Nand Mishra, Sharmila, Apranjal Singh, Chetan Barde, Wide angle metamaterial absorber for S, C and X band application, Frequenz 78 (1–2) (2024) 21–29, https://doi.org/10.1515/freq-2022-0283.

[35] S. Hannan, M.T. Islam, A.F. Almutairi, M.R.I. Faruque, Wide bandwidth angle- and polarization-insensitive symmetric metamaterial absorber for X and Ku band applications, Sci. Rep. 10 (1) (Dec. 2020), https://doi.org/10.1038/s41598-020-67262-5.

[36] S. Hossen, Md K. Uddin, A. Gafur, S. Zahidur Rashid, S. Hannan, A.Z.M. Imran, Design and analysis of an antenna using ring slotted rectangular reflector with double substrate for 5G mm-wave application, in: 2023 International Conference on Next-Generation Computing, IoT and Machine Learning (NCIM), 2023, pp. 1–6, https://doi.org/10.1109/NCIM59001.2023.10212444.